

# ***UBV(RI)<sub>c</sub>* photometry and spectroscopy of the young open cluster Haffner 19**

Ulisse Munari<sup>1</sup> and Giovanni Carraro<sup>2</sup>

<sup>1</sup>*Osservatorio Astronomico di Padova, sede di Asiago, 36012 Asiago (VI), Italy*

<sup>2</sup>*Dipartimento di Astronomia, Università di Padova, vicolo dell'Osservatorio 5, I-35122, Padova, Italy*

Accepted 1996 July 16. Received 1996 July 8; in original form 1995 December 7

## **ABSTRACT**

We present accurate CCD photometry in the *UBV(RI)<sub>c</sub>* bands of a  $2.9 \times 2.4$  arcmin<sup>2</sup> field centred on the young open cluster Haffner 19. Spectral types for 4 members are derived from CCD spectroscopy. 64 probable cluster members are identified down to  $V=18.1$ .

The cluster lies at 5.0 kpc and suffers from a marked differential reddening [ $\Delta E(B-V)=0.5$ ] with a mean value  $E(B-V)=0.44$ . The extinction law conforms well to the one valid for the diffuse interstellar medium ( $R_V=3.1$ ). The main sequence is well defined over the 7-mag interval we explored, with spectral types B0 and F8–G0 on the sequence. The fit with theoretical isochrones gives an age of about  $6 \times 10^6$  yr.

**Key words:** Hertzsprung–Russell (HR) diagram – open clusters and associations: individual: Haffner 19.

## **1 INTRODUCTION**

Haffner 19 ( $\alpha_{2000}=7^{\text{h}}52^{\text{m}}7$ ,  $\delta_{2000}=-26^{\circ}15'$ ,  $l=2430$ ,  $b=+0^{\circ}5$ ) lies in a direction of low interstellar extinction in Puppis, where OB associations (Pup OB1 and OB2), H II regions (S311) and field OB stars are found. This is also the region of NGC 2467, a former open cluster now recognized to be just a chance alignment of the above components.

Investigations of Haffner 19 and the surrounding field have been presented by FitzGerald & Moffat (1974, hereafter FM), Reed & FitzGerald (1983), Feinstein & Vazquez (1989) and Labhardt, Spaenhauer & Schwengeler (1992, hereafter LSS); none of them, however, deal with the crowded central region of the cluster. It has been suggested that Haffner 19 (a) lies at  $\sim 7$  kpc from the Sun, beyond Pup OB1 and OB2 (it could be part of a spiral arm in the galactic anti-centre direction at 15 kpc, associated with the Perseus arm extension); (b) has a mean  $E(B-V)=0.45$ , normal extinction law and differential reddening; and (c) is young (from 4 to 8 million years), having the earliest spectral type (B0).

In this paper, we report *UBV(RI)<sub>c</sub>* CCD photometry of Haffner 19, when more and fainter are measured compared to previous studies and the central crowded region is spatially resolved. CCD spectra are presented for four cluster stars.

**Table 1.** Journal of observations. Seeing is the FWHM of stellar images as measured on the CCD frames.

Date	Filter	Exp. time (sec)	Seeing ( $''$ )
Feb. 28, 1992	R	10	1.1
	I	15	0.9
	I	25	0.8
	R	20	1.0
	V	40	1.1
	B	120	1.2
	B	40	1.2
	U	60	1.2
	U	600	1.3
	B	900	1.2
	V	720	1.0
	R	360	0.9
	I	600	0.9

## 2 PHOTOMETRY

Photometry of Haffner 19 has been carried out with the CCD camera mounted on the 1.0-m telescope of the South Africa Astronomical Observatory (SAAO) at Sutherland on 1992 February 28. The same night, we observed the young open cluster Bochum 2 on which we have reported elsewhere (Munari & Carraro 1995a, hereafter MCA), together

with a detailed instrumental evaluation and observation/data reduction procedures. The reader is referred to MCA for the observational details. The photometry here presented is strictly tied onto the Cousins' standards in the southern E-regions.

The journal of observations is given in Table 1 and the resulting  $UBV(RI)_c$  magnitudes in Table 2. A finding chart is presented in Fig. 1, where the crowded central region is

**Table 2.**  $UBV(RI)_c$  photometry of Haffner 19. Columns gives our running number, those of FM and LSS, the X and Y positions on the chip (to be compared with Fig. 1 for identification), and the  $UBVRI$  magnitudes and associated internal errors (in millimag) as given by the DAOPHOT package.

Star	FM	LSS	X	Y	V	$\sigma_V$	B-V	$\sigma_{B-V}$	V-I	$\sigma_{V-I}$	V-R	$\sigma_{V-R}$	U-B	$\sigma_{U-B}$
1			272.03	5.14	14.638	9	0.622	10	0.698	14	0.358	16	0.185	21
2			9.22	21.30	16.830	10	0.876	17	0.991	16	0.462	20		
3			260.67	34.15	16.944	11	0.709	16	0.761	19	0.397	17		
4			119.18	57.43	16.834	9	0.813	16	0.884	14	0.403	16		
5			206.07	84.44	16.138	9	1.020	13	1.122	13	0.562	13		
6			86.35	129.50	16.462	6	0.835	12	0.887	10	0.439	13		
7			69.72	182.35	16.361	9	0.461	11	0.582	14	0.261	13		
8		11	108.57	201.26	16.818	8	0.995	15	1.043	12	0.505	14		
9	4031	29	189.01	205.09	15.642	6	0.744	9	0.964	11	0.479	10		
10	4030	31	217.31	214.63	14.909	4	0.504	5	0.583	6	0.229	9		
11			293.76	222.59	17.026	11	0.693	17	0.823	20	0.389	19		
12	4033	28	180.61	229.88	16.005	18	0.495	19	0.536	21	0.199	13		
13		24	162.68	243.54	15.412	6	0.468	8	0.420	10	0.149	11		
14		32	224.33	249.55	16.267	5	0.369	8	0.546	10	0.225	9		
15	4029	33	232.50	257.61	15.736	6	0.674	8	0.744	10	0.355	11		
16		30	195.13	257.83	16.751	9	0.566	13	0.615	13	0.261	14		
17		3	51.92	258.83	16.310	7	0.524	9	0.586	11	0.235	11		
18	4028	34	241.52	261.09	14.445	4	0.521	4	0.682	8	0.306	10	0.431	18
19	4034	26	176.62	282.96	15.697	8	0.656	11	0.753	14	0.333	14		
20	4035	27	177.72	326.58	15.204	6	1.265	9	1.344	12	0.697	12		
21		21	151.73	335.37	16.524	7	0.703	11	0.820	14	0.621	29		
22	4023	38	291.36	351.63	14.567	3	0.321	4	0.395	8	0.175	10	-0.081	12
23		9	87.36	361.15	16.769	9	0.770	16	0.853	13	0.383	17		
24	4037	16	133.96	370.82	14.525	5	0.280	6	0.306	9	0.140	7	-0.036	13
25	4024	40	300.47	382.38	13.113	4	1.381	4	1.345	23	0.683	16		
26	4026	35	246.19	391.24	15.182	7	0.648	8	0.792	10	0.353	11		
27	4040	2	45.24	401.36	16.296	13	0.603	17	0.725	20	0.346	20		
28		37	279.35	402.70	16.974	7	0.780	14	0.868	15	0.423	12		
29		39	298.57	410.09	16.335	8	0.507	11	0.620	12	0.262	13		
30			162.44	410.81	16.313	6	0.438	10	0.494	12	0.199	13		
31			242.73	465.36	15.950	7	0.383	8	0.456	14	0.189	16		
32	4041		124.58	478.21	15.645	5	0.489	6	0.587	11	0.237	13		
33			27.10	92.93	15.594	9	0.547	10	0.642	11	0.294	13		
34	4055	22	153.98	242.01	14.332	6	0.388	7	0.457	8	0.189	9	0.012	12

Table 2 – continued

ID	FM	LSS	X	Y	V	$\sigma_V$	B-V	$\sigma_{B-V}$	V-I	$\sigma_{V-I}$	V-R	$\sigma_{V-R}$	U-B	$\sigma_{U-B}$
35		19	142.50	268.51	15.568	5	0.472	8	0.523	9	0.216	10		
36			133.27	295.27	15.985	9	0.507	15	0.489	15	0.207	15		
37		5	62.24	299.96	16.447	6	0.482	9	0.480	11	0.198	12		
38	4049	8	77.18	322.49	15.085	5	0.350	6	0.383	7	0.159	9	0.077	19
39	4027	36	259.40	325.91	15.519	4	0.658	6	0.680	8	0.345	9		
40	4038	10	95.93	393.72	15.118	7	0.292	8	0.356	11	0.167	9		
41			253.89	487.42	17.068	11	0.587	16	0.777	16	0.325	17		
42			252.61	496.71	15.110	5	0.758	6	0.812	11	0.437	12		
43			19.74	3.97	16.343	10	0.556	12	0.706	16	0.357	12		
44			153.60	88.51	16.251	9	0.635	15	0.722	14	0.358	14		
45	4047	7	74.41	261.42	14.654	4	0.401	6	0.528	11	0.204	10	-0.074	14
46	4036	25	168.25	392.23	14.549	4	0.688	8	0.757	8	0.360	10		
47			215.11	472.69	16.523	8	0.585	13	0.715	14	0.324	12	0.296	21
48	4032	20	150.94	174.93	13.970	6	1.227	7	1.249	10	0.630	11		
49	4039	6	71.36	402.61	15.885	6	0.356	9	0.384	10	0.159	13		
50	4053	18	142.10	248.65	13.109	7	0.305	8	0.373	11	0.160	11	-0.279	6
51	4048	4	54.90	289.28	15.477	7	0.376	9	0.417	10	0.170	9		
52		15	124.59	295.08	14.265	9	0.328	11	0.369	17	0.165	16	-0.173	11
53	4052	12	114.61	272.97	12.824	9	0.318	11	0.353	18	0.160	16	-0.258	8
54	4020	41	304.83	226.16	14.365	6	1.321	8	1.452	13	0.787	13		
55			114.55	289.00	13.473	15	0.273	19	0.403	23	0.319	82	-0.324	75
56	4050	17	136.14	308.56	12.343	12	0.266	13	0.267	16	0.121	14	-0.301	6
57	4045	1	16.33	354.91	12.323	10	0.173	12	0.206	14	0.100	17	-0.355	15
58	4042		156.05	507.10	16.175	6	0.548	12						
59			120.24	266.79	14.649	8	0.588	11	0.615	14	0.282	15		
60	4051	14	120.04	285.70	11.156	2	0.248	4	0.263	7	0.114	20	-0.329	20
61			251.11	233.99	17.368	21			0.920	21	0.442	16		
63			11.49	242.33	18.096	25			1.209	16	0.637	25		
63			3.63	301.07	17.447	12			0.876	18	0.422	18		
64			25.03	291.55	18.049	20			1.552	22	0.779	24		
65			101.36	318.22	17.668	15			1.272	21	0.618	23		
66			141.96	190.72	17.424	12			1.020	16	0.507	16		
67			124.47	238.06	17.808	13			0.968	24	0.433	25		
68			144.69	317.33	17.654	11			1.525	37	0.739	35		

re-plotted in the upper-left corner for easier identification.

Comparison between our profile CCD photometry and the photoelectric aperture photometry of FM gives (26 stars in common)

$$V - V_{FM} = 0.032, \sigma = 0.129 \quad (1)$$

$$(B - V) - (B - V)_{FM} = 0.214, \sigma = 0.189. \quad (2)$$

The agreement is much better defined with the CCD aperture photometry of LSS, for which is found (37 stars in common)

$$V - V_{LSS} = -0.032, \sigma = 0.031 \quad (3)$$

$$(B - V) - (B - V)_{LSS} = 0.047, \sigma = 0.029. \quad (4)$$

Our photometry is in the 0.064-map gap (in  $V$  and similarly in the other colours) between the results of LSS and

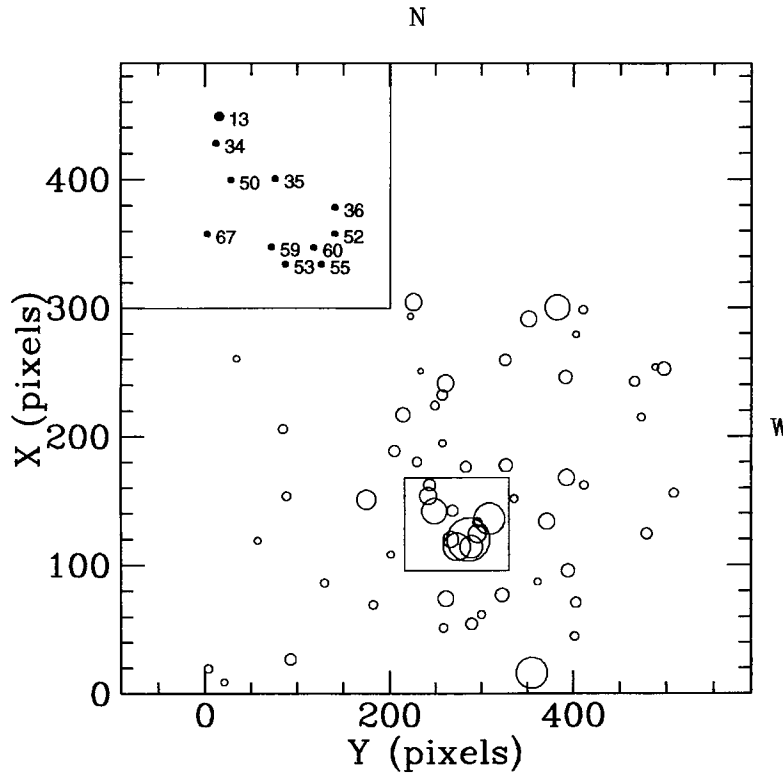


**Figure 1.** Identification map. The imaged field covers  $2.4 \times 2.9$  arcmin<sup>2</sup>. The crowded central region has been enlarged (upper-left corner) for easier identification.

FM. The comparison with FM and LSS photometry is shown in graphical form in Fig. 2. No systematic trend with colour or magnitude is evident. We can confirm the LSS conclusion that the large scatter and offset of the FM photoelectric aperture photometry is traceable to contamination from fainter field stars entering the diaphragm. The small difference between our and LSS results could be partially ascribed to different sets of standards and software packages used (Cousins' E-regions and DAOPHOT for us, Landolt's equatorial standards and ROMAPHOT for LSS).

FM suggested that star N19 may be variable. However, our photometry gives  $V=15.697$ , in close agreement with the  $V=15.60$  reported by FM.

### 3 SPECTROSCOPY

A long-slit spectrum of Haffner 19 was obtained for us by A. Bragaglia (Astronomical Observatory of Bologna, Italy) on 1994 February 25, with the B&C and CCD spectrograph mounted on the ESO 1.5-m telescope. The wavelength range covered is from 3380 to 9190 Å, with a dispersion of  $2.5 \text{ Å pixel}^{-1}$  and a resolution of  $\sim 7 \text{ Å}$ . The slit was oriented to record simultaneously the spectra of stars 34, 50, 53 and 57. In Fig. 3 we present an expanded plot of the spectra over the standard region for spectral classification.

Spectral types are reported in Table 3, together with derived colour excesses from comparison with the tabular values listed by FitzGerald (1970) and Bessell (1990). The classification of star number 60 is taken from FM.

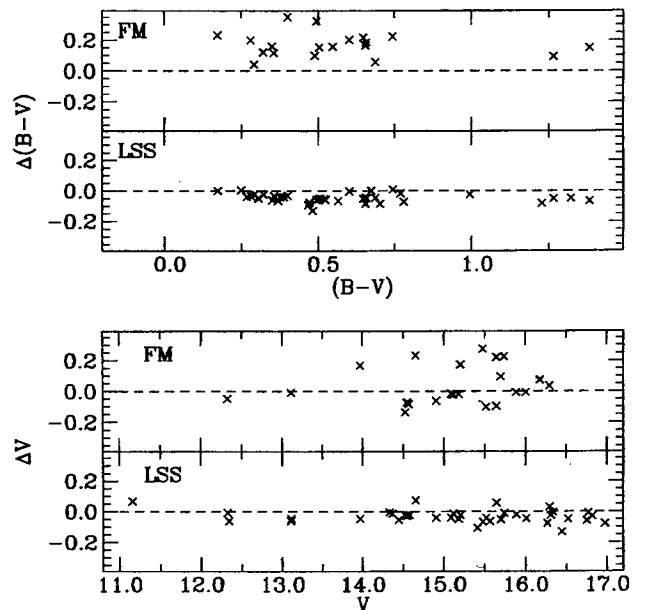


**Figure 2.** Comparison between FM, LSS and our photometry for the stars in common.

### 4 RESULTS

The  $V-(B-V)$  and  $V-(V-I)$  diagrams for the stars reported in Table 2 are shown in Fig. 4. The main sequence appears well defined over a range of 7 mag, down to spectral type F8 – G0 (for the cluster distance and reddening

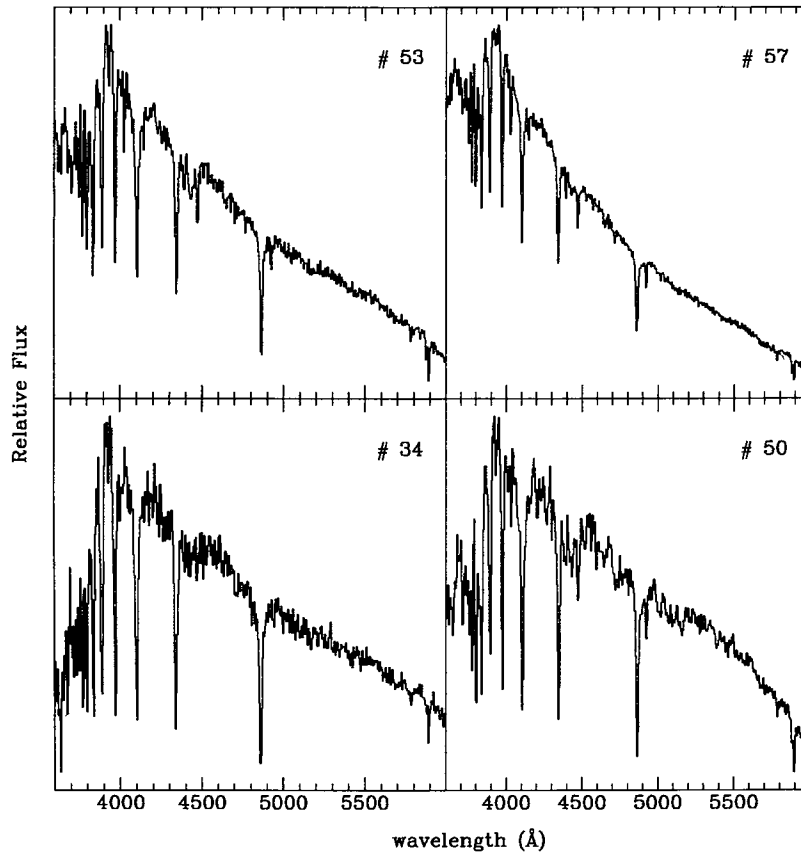


Figure 3. Enlarged section of the CCD spectra for stars 34, 50, 53 and 57.

**Table 3.** Spectral classification from slit spectra. The classification for star number 60 is from FitzGerald & Moffat (1974).

Star #	Type	$E_{B-V}$	$E_{U-B}$	$E_{V-R}$	$E_{V-I}$
34	B7 V	0.52	0.44	0.22	0.54
50	B3	0.49	0.40	0.23	0.54
53	B2 V	0.56	0.55	0.23	0.52
57	B2 V	0.43	0.46	0.17	0.38
60	B0 V	0.55	0.75	0.21	0.47

derived below). No evolved star is detected as a cluster member. Only four stars, identified in Fig. 4, depart clearly from the main sequence. Lying away from the cluster centre, they are quite possibly field stars. The remaining 64 stars in Table 2 look much like cluster members.

We observed two stellar fields away from the cluster to statistically evaluate the amount of contamination from field stars. Unfortunately, the entire region around Haffner 19 looks very patchy even on the ESO sky survey prints, with many dust lanes running through the field. The latter also affected the two stellar fields we observed, and therefore a careful statistical evaluation of the contamination cannot be performed. A rough guess based on simple stellar counts

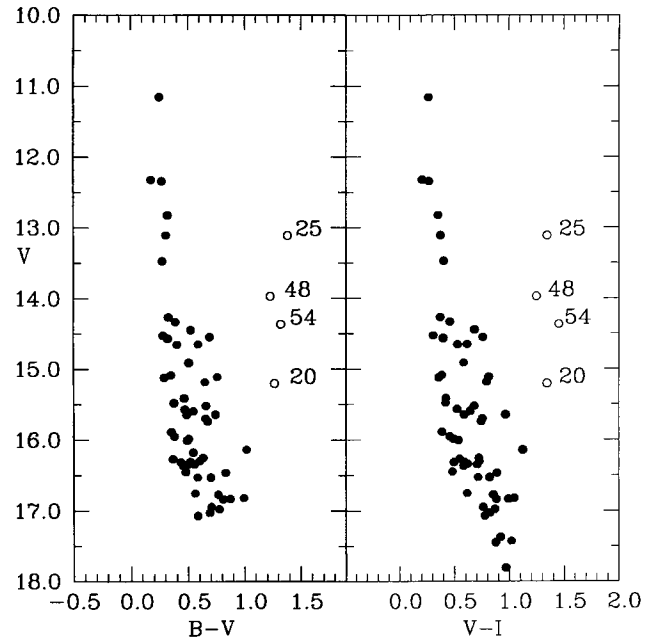


Figure 4. Haffner 19 in the  $V-(B-V)$  (left panel) and  $V-(V-I)$  (right panel) planes from photometry in Table 2.

per bin of magnitude suggests a contamination not exceeding 7 stars over the entire Haffner 19 region we imaged, i.e. not more than 3 field stars being overimposed on the cluster main sequence in Fig. 4. This is confirmed by the sharpness

of the main sequence in Fig. 4 (particularly at the bottom of both diagrams) and by how well the four field stars are separated from it.

The broadness of the main sequence does not increase with magnitude. This suggests that at the chosen cut-off ( $V \leq 18.1$ ) for the inclusion of measured stars in Table 2, the photometry is still only marginally affected by errors and the most likely cause of the main sequence broadness is the strong differential reddening across the cluster, with possible minor contribution from the crowding (pairs of stars merging into a single one at the 1.0-arcsec resolution of our imaging). From the width of the main sequence, after allowing for a  $\sigma^2(B-V) = 0.03$  spread induced by photometric errors (cf. column 9 in Table 2), it can be estimated that the differential reddening across the cluster amounts to  $\Delta E(B-V) = 0.5$  mag.

We derived a reddening map for the cluster (see Fig. 5), computing individual reddening for the stars (14) with  $U-B$  available and adopting the colour ratio given by equation (6) (see below). It is difficult to distinguish any trend in the reddening map. Assuming, for instance, a linear decrease of the reddening from a value of 0.70 in the north-east to a value of 0.35 in the south-west does not lead to a cleaner CMD. In any case, we obtained a  $V_0 - (B-V)_0$  plot for these 14 stars, that actually shows a tighter MS.

We have performed trial fits of the main sequence with theoretical isochrones of the Padova group (cf. Bertelli et al. 1994), characterized by a standard  $[\text{He}/\text{H}]$  ratio and  $Z = 0.020$ . The best fit (see Fig. 6) is obtained for the isochrone corresponding to the age of  $6 \times 10^6$  scaled to  $E(B-V) = 0.44 \pm 0.03$  and  $(m-M)_0 = 13.54 \pm 0.08$  (equivalent to 5.1 kpc). This result has been obtained considering all the most luminous stars as MS stars, according to their spectral type (see Table 3).

For each of the 5 cluster members spectroscopically classified in Table 3, the usual distance modulus formula can be written as:

$$(V-M_V)_i = 5 \log d - 5 + R_V[(B-V) - (B-V)_0] \quad (5)$$

Using a least-squares solution it is possible to derive the value of  $R_V$  and the cluster distance simultaneously, once absolute magnitudes are assumed. We adopted those listed by Schmidt-Kaler (1982). It is found that  $d = 4.7$  kpc and  $R_V = 3.15$ . The distance is in excellent agreement with the fit to theoretical isochrones and in our opinion definitively rules out the much greater distance reported by FM ( $6.9 \pm 0.9$  kpc). The extinction law obeys the relation for the diffuse interstellar medium, characterized by  $R_V = 3.1$  (Mathis 1990).

The normality of the extinction law can be also guessed by the ratios of the colour excesses reported in Table 3 compared with those derived by Munari & Carraro (1995b, hereafter MCb) from the Mathis (1990) extinction law for the case  $R_V = 3.1$  (in square brackets):

$$\frac{E(U-B)}{E(B-V)} = 0.93 \quad [0.82], \quad (6)$$

$$\frac{E(V-R)}{E(B-V)} = 0.44 \quad [0.54], \quad (7)$$

and

$$\frac{E(V-I)}{E(B-V)} = 1.04 \quad [1.25]. \quad (8)$$

Recently, Natali et al. (1994) suggested the use of a linear

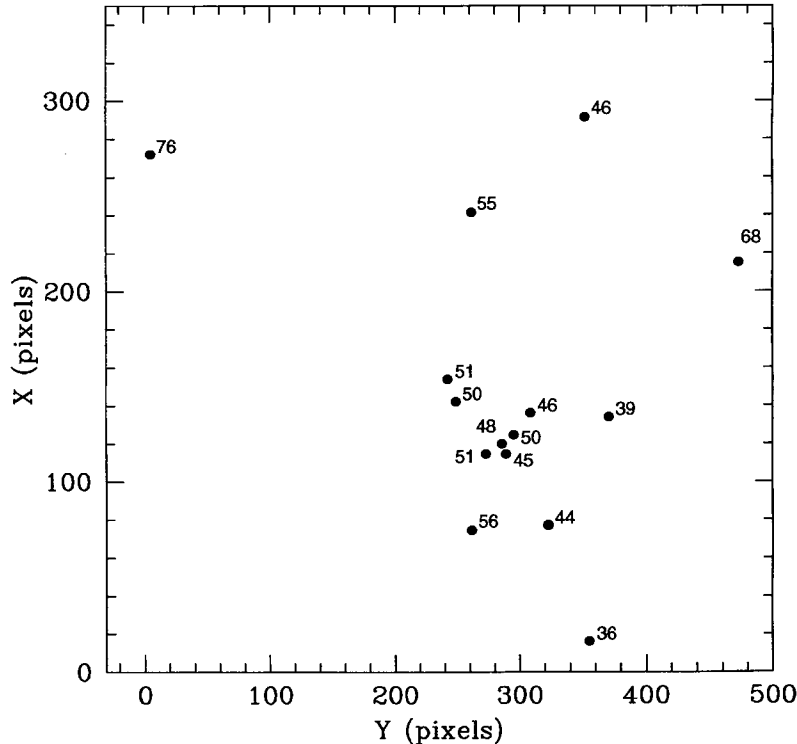


**Figure 5.** Reddening map for Haffner 19. The numbers correspond to  $100 \times E(B-V)$ .

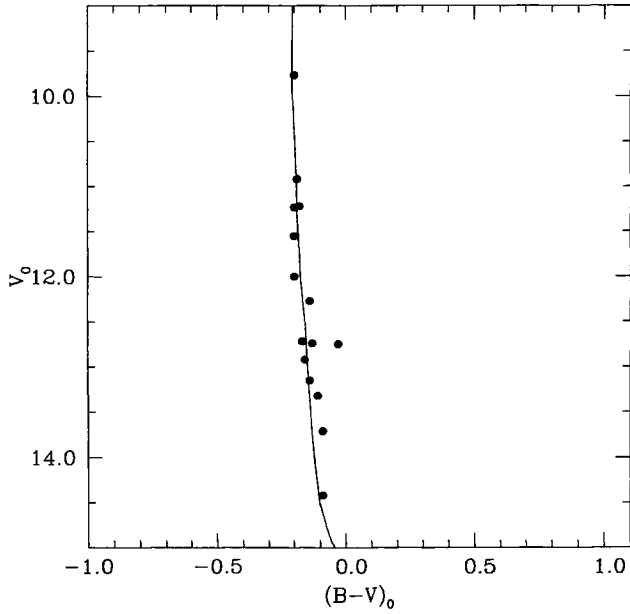


**Figure 6.** CMD of Haffner 19 for the 14 dereddened stars. Over-imposed is a solar composition isochrone for an age of  $6 \times 10^6$  yr (Bertelli et al. 1994).

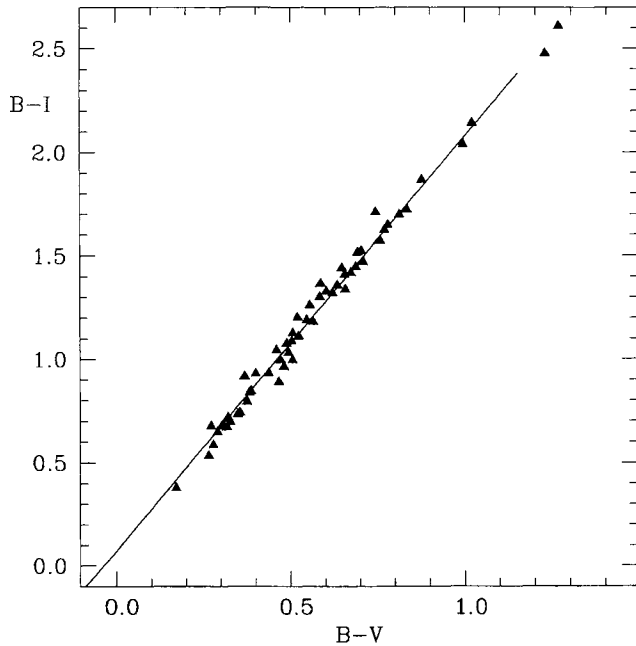


**Figure 7.** Haffner 19 stars in the  $(B-I) - (B-V)$  plane.

fit to the cluster main sequence to estimate the reddening in the  $B-V$ ,  $B-I$  plane. The method has been revised by MCb who pointed out some discrepancies in the Natali et al. formulation. The linear fit to the main sequence in the  $B-V$ ,  $B-I$  plane,

$$(B-I) = Q + 2.25(B-V), \quad (9)$$

can be expressed in term of  $E(B-V)$  for the  $R_V=3.1$  extinction law as

$$E(B-V) = \frac{Q - 0.014}{0.159}. \quad (10)$$

For the 64 probable cluster members in Table 2, the fit is presented in Fig. 7. It gives  $Q=0.081$  which translates into  $E(B-V)=0.42$  in excellent agreement with the above determination [ $E(B-V)=0.44$ ] from the fit with the theoretical isochrone and the  $E(B-V)=0.45$  reported by FM. Using the original formulation by Natali et al. would have resulted in  $E(B-V)=0.28$ .

#### ACKNOWLEDGMENTS

This work has been financially supported by the Italian Ministry of University, Scientific Research and Tecnology (MURST) and the Italian Space Agency (ASI).

#### REFERENCES

- Bertelli G., Bresan A., Chiosi C., Fagotto F., Nasi E., 1994, A&AS, 106, 275
- Bessell M. S., 1990, PASP, 102, 1181
- Feinstein A., Vazquez R. A., 1989, A&AS, 77, 321
- FitzGerald M. P., 1970, A&A, 4, 234
- FitzGerald M. P., Moffat A. F. J., 1974, AJ, 79, 873 (FM)
- Labhardt L., Spaenhauer A., Schwengeler H., 1992, A&A, 265, 869 (LSS)
- Mathis J. S., 1990, ARA&A, 28, 37
- Munari U., Carraro G., 1995a, MNRAS, 277, 1269 (MCa)
- Munari U., Carraro G., 1995b, A&A, in press
- Natali F., Natali G., Pomepi E., Pedichini F., 1994, A&A, 289, 756
- Reed C. B., FitzGerald P. M., 1983, MNRAS, 205, 241
- Schmidt-Kaler Th., 1982, in Schaifer K., Voigt H. H. eds, Landolt-Börnstein, Numerical Data and Functional Relationships in Science and Technology. New Series, Group IV, Vol. II. Springer, Berlin, p. 14